Smart equipment failure detection with machine learning applied to thermography inspection data in modern power systems

Ana María Garzón[1],*Student Member, IEEE*, Natalia Laiton[1],*Student Member, IEEE*, Victor Sicachá[1], *Student Member, IEEE*, David F. Celeita[1], *Senior Member IEEE* and Trung Dung Le[2]
[1] Universidad del Rosario, School of Engineering, Science and Technology, Bogotá, Colombia
[2] Université Paris-Saclay, CentraleSupélec, CNRS, Group of Electrical Engineering Paris (GeePs), Gif-sur-Yvette, France.

***Abstract*—This paper presents a novel approach to detecting equipment failures in modern power systems by leveraging machine learning techniques applied to thermography inspection data. Particularly segmentation and pixel processing to improve accurateness is highlighted in the methodology. The proposed method is capable of identifying early warning signs of equipment failure and predicting when the failure is likely to occur. The proposed approach demonstrates the potential for early detection of equipment failure in modern power systems with accurate clustering. The use of machine learning algorithms applied to thermography inspection data provides a reliable and effective way to identify and predict equipment failures, ultimately leading to improved system reliability and reduced maintenance costs.**

***Index Terms*—Thermography inspection, image segmentation, predictive fault identification, machine learning, neural network.**

I. Introduction

As power systems become increasingly complex, the reliable and efficient operation of smart equipment has become critical for ensuring continuous power supply [1]. The failure of critical components in such equipment can have severe consequences, including power outages, safety hazards, and significant financial losses. To mitigate these risks, the use of machine learning techniques for equipment failure detection has gained traction in recent years [2], [3]. In particular, thermography inspection data provide valuable insights into the operating conditions of smart equipment [4], which can be leveraged to develop accurate predictive models.

Predictive maintenance is an essential part of keeping the efficiency and reliability of power equipment, and machine learning has emerged as a powerful tool for this task. In particular, machine learning with thermography images has shown promise for detecting potential equipment failures before they occur [5]. Thermography is a non-destructive and non-intrusive testing technique that measures the temperature of an object using infrared radiation. By analyzing thermography images of power equipment, machine learning algorithms can detect patterns and anomalies that may indicate potential equipment failures.

Some studies propose deep learning approaches for detecting and diagnosing faults, for example in photovoltaic systems using thermographic images [6]. In [7] a two-stage approach, where the first stage involves identifying potential faults using a convolutional neural network (CNN), and the second stage involves diagnosing faults using a residual neural network (ResNet).

In [8] there is the introduction to a new dataset for fault diagnosis in electrical equipment using thermal imaging. The study integrates an interpretable machine learning approach that combines decision trees with feature selection and feature importance ranking methods to diagnose faults in electrical equipment.

The review presented in [9] compiles the studies where infrared thermography is used for energy audits of buildings. In most of the reviewed references, experimental results show that the proposed approaches achieves high accuracy in detecting and diagnosing faults. In overall, these studies demonstrate the potential of using thermal imaging and deep learning for fault diagnosis in photovoltaic systems [10] and energy audits in residential or commercial buildings.

Machine learning can be a powerful tool for predictive maintenance in power equipment when combined with thermography images. To use machine learning for predictive maintenance with thermography images, a dataset of thermography images must be first collected and labeled according to the condition of the equipment at the time the image was taken. The images must then be preprocessed to remove noise and ensure consistency. Next, a machine learning model can be trained on the preprocessed data using a variety of algorithms, such as support vector machines, random forests, or neural networks. The choice of algorithm will depend on the specific requirements of the application. Once the model has been trained, it can be used to predict the condition of the equipment based on new thermography images. This allows for timely maintenance to be performed before equipment failure occurs, thereby reducing downtime and maintenance costs.

In this paper, we present a novel approach to equipment failure detection using machine learning applied to thermography inspection data. We demonstrate the effectiveness of our approach through a case study on a modern power system, highlighting the potential for improved reliability and reduced downtime in smart equipment operations. This paper is organized as follows: section II defines the Types

of Thermographic Inspections in power systems. In section III, a detailed description of the proposed methodology is presented. It comprises three main stages: data acquisition, feature extraction, and machine learning-based classification. The data acquisition stage involves capturing thermal images of equipment under inspection, which are then processed to extract relevant features. These features are then fed into a machine learning algorithm, which classifies given the temperature of normal or abnormal thresholds. Then, the algorithm's testing and the findings achieved in the case study is presented in section IV. Some conclusions and perspectives are given in section V.

II. Types of thermographic inspection of power systems

When carrying out a literaturel review of the monitoring of power systems with IR images, it is possible to notice that there are two types of images: images obtained in closed spaces and images obtained in open spaces. Such classification is proposed on our approach (see Fig. 1) to objectively categorized the methods depending on the physical environment of the power system equipment.

Those located in open spaces typically monitor solar panels and photovoltaic cells, or electrical transmission lines. The images are taken either by locating the camera in drones, or in a high or distant fixed point.

Two points must be considered in the preprocessing of these images: The first is the distinction of the background from the system or equipment to be monitored. Unlike the images that are taken in closed spaces, it must be considered that in this case the light and the temperature of the environment are variable and impossible to control. Thermal imaging cameras are sensitive to these factors which can make segmentation more difficult. On the other hand, the perspective in which the images have been taken is also an important point in their preprocessing.

The second point of the preprocessing is the distinction of the parts or regions of interest for monitoring once the background has been separated: In the case of solar panels, it is convenient to obtain information from each photovoltaic cell separately, for example, and this requires additional work.

On the other hand, monitoring in closed spaces is typically carried out under constant ambient temperature and lighting conditions, which allows a better generalization to be made to distinguish the object from the background. Under this condition, simple systems, such as a single motor or transformer, or complex compound systems that include multiple machines can be monitored. In the second case, in addition to distinguishing the region of interest from the background, it is necessary to identify the different parts of the image to obtain a localized and accurate prediction.

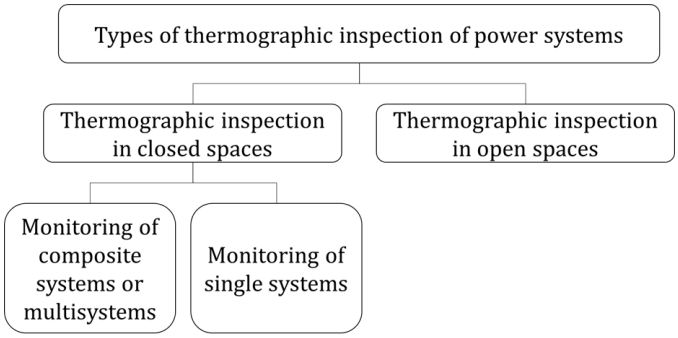

Fig. 1. Types of thermographic inspection of power systems

III. Methodology

For the identification of failures, the same process is carried out both in monitoring in open spaces and in closed spaces. As illustrated in Fig. 2 The first step is to obtain images of the equipment to be inspected using an Infrared (IR) camera at the appropriate distance and angle.

The second step is the pre-processing of the image data, which allows obtaining information from the images and being able to introduce them into a segmentation or ML algorithm. This preprocessing includes converting the image files to a format that allows working with the image pixel by pixel; a vectorization of the image to be able to introduce it into the algorithms, then the selection of the appropriate color space; the use of filters, morphological changes or contrast depending on the case.

Next, the identification of the Region of Interest (RoI) is done. This segmentation can be done by hand by an expert, which is convenient in cases where neither the camera nor the power system has position changes; or it can be automated, and this automation can be a more or less precise segmentation according to the needs. This process is crucial because it has a direct impact on the performance of the next step: classification or identification of the failure.

This last point is based on the implementation of an ML algorithm, supervised, unsupervised, or by reinforcement, on the region of interest, which incidentally identifies if the system has a fault, and if so, identifies the type of fault.

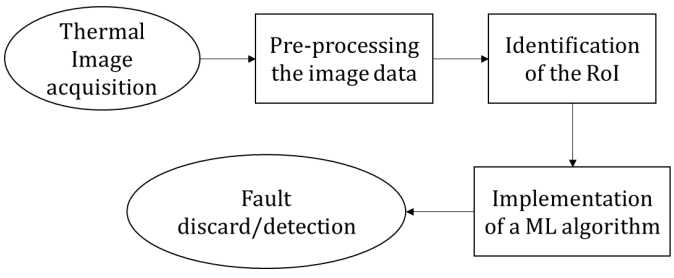

Fig. 2. Steps for automated detection of faults in power systems using IR images

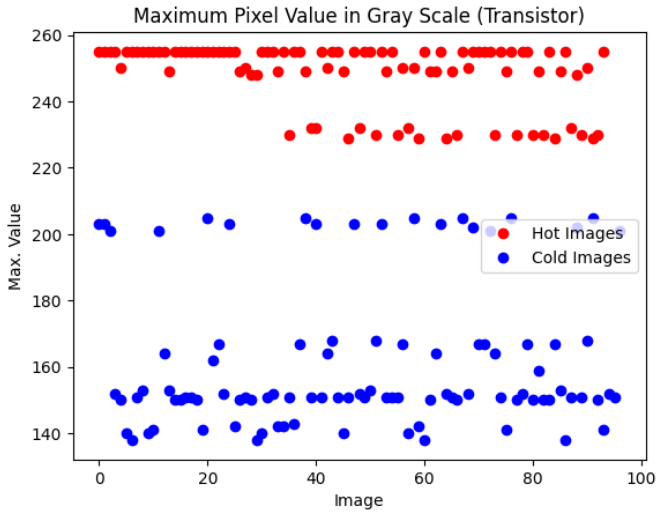

Fig. 3. Maximum Pixel Value (Transformer)

IV. Case study description: closed space, single system

In this paper, the procedure carried out in [8] is analyzed, implemented, and modified, using the dataset created for that case study. The dataset consists of 624 thermal images of 320x240 pixels, of which 369 correspond to images of induction motors and 255 to images of transformers. The images were taken by a Dali-tech T4/T8 infrared thermal image camera at 23° Celsius of environment temperature.

Regarding the transformer, 8 cases of short circuit failures in common core winding are taken into account to generate the defects artificially; while 8 different cases of artificial generated stuck rotor fault, cooling fan failure and stator windings failure are considered.

The objective of both the investigation carried out by the researchers and by the present manuscript is to find the best way to distinguish and classify the failures described above.

A. Data Preprocess

The first step on this path is the pre-processing of the data. The images are converted to grayscale, a projection of RGB space in which each pixel takes a single value from 0 to 255, instead of taking 3 different component values. The advantage of working in grayscale is that this dimensionality reduction decreases the time and computational cost of the algorithms. Regarding the temperature, this is directly proportional to the pixel value. However, it should be considered that this reduction could lead to loss of information.

[8] proposes to classify ”cold” and ”hot” images before segmenting the region of interest and the same will be done here. To carry out the classification, the data was divided into training and test sets, the pixels with the highest value from each of the images were extracted, and the behavior of these values in the training set was explored.

In Fig. 3 it is noticeable that there is a clear difference between the maximum value of the cold images and the hot images. Similar results are obtained for the motor. To perform a classification, use intermediate values (mean or median) to generate a classification threshold, establish a threshold through observation, or use a support vector machine classification that finds a hyperplane (or line) that conditions the classification.

The results obtained when using linear SVM are a perfect classification for both cases (which is not surprising since the classes are quite distant). However, from the plot of the train data, it is evident that the data is grouped in more than two subgroups focusing only on the maximum value pixel. In this sense, additional exploration of the dataset is done with KMeans, trying to distinguish those subgroups and the number of clusters is determined through the elbow method. For both the transformer and the motor the optimal number of clusters is 5; 3 clusters for cold images and 2 clusters for hot images as shown inf Fig. 4.

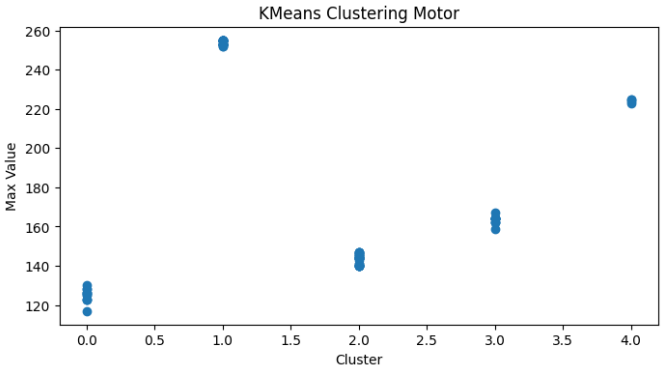

Fig. 4. K means

By comparing the results obtained above with the failure that corresponds to each value, it is noticeable that the images that have the same fault label often are located in the same cluster. It can be inferred that the maximum value pixel is a good guide not only to create an effective preprocessing that facilitates the segmentation of the region of interest but also to approximate the final classification.

B. Identifying RoI (Region of Interest)

From the previously identified clusters, an image is chosen at random from each of the previous groups to create a manual mask of the region of interest, which will allow evaluation of the results obtained by the automation.

The segmentation challenge, in this case, is that the images were taken at different angles, on a surface that reflects the light emitted by the equipment, and that includes cables external to the equipment that should be included in the RoI since they provide information about the state of the phases.

In this sense, the algorithm to find the RoI follows the following steps:

C. *Initial segmentation setting a threshold:*

Segmentation of an image in two regions can be done by setting a threshold k such that if a pixel has a value that is greater than k it belongs to a class and if not, it belongs to the other. The threshold can be defined manually or by numerical methods by identifying inflection, local maximum, or minimum points in the histogram of the distribution of pixel intensity.

However, it is a nonoptimum procedure on a large scale. Then, a threshold function $f(x, y)$ must be defined such that if a pixel with coordinates (x, y) evaluated in f has a value greater than k belongs to one region R_1, and if the value is less or equal to k it belongs to the other region R_2. This procedure can be summarized by the following function:

$$g(x,y) = \begin{cases} 1 \quad if \quad f(x,y) > k \\ \\ 0 \quad if \quad f(x,y) \leq k \end{cases} \tag{1}$$

The problem now consists of finding the most optimal and general function f and the threshold k. As explained in [11], it has been sought to use a PDF probability density function, but the limitation is that the calculation of functions requires many distribution assumptions that are not always fulfilled and cannot be easily calculated for atypical distributions.

A solution to this problem exposed by the same source [11], is OTSU's method. It is an optimum procedure where f maximizes the variance between classes, basically carrying out a statistical method of discriminant analysis on the intensity of the pixels. An advantage of the OTSU's method highlighted by the authors is that its results are obtained from the histogram giving, as a result, an array of dimension 1. Access the complete process and the specifications of the OTSU formulas in the following repository: https://github.com/anamarigarzon/IR-Image-Analysis-in-Power-Systems

In this project, the cluster to which the image belongs is considered. Similar and satisfactory results are usually obtained for hot images by applying OTSU directly. For cold images, a histogram equalization procedure is performed, which standardizes the image values, some morphological erosion transformations and finally OTSU is applied.

There are multiple ways of finding this threshold function, which vary depending on the image distribution. A useful and simple but very manual way to establish it is to plot the histogram of the distribution of the pixel values in the image and determine possible segmentation points.

D. *Shadow elimination and addition of the missing equipment area:*

Next, a new OTSU segmentation is performed on the portion of the image that is outside the mask obtained in the previous step. In the images of the two clusters with a smaller maximum pixel value, the problem is that the equipment section has a temperature very close to that of the background, so it is advisable to perform morphological operations and extra contrast enhancement to increase differentiation.

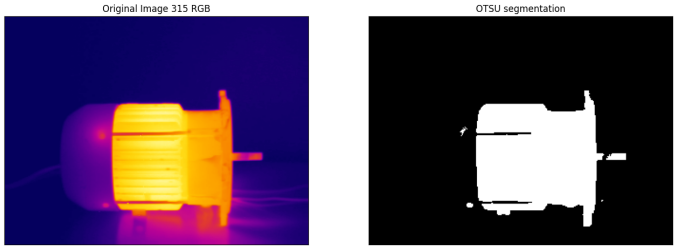

Fig. 5. Example of Initial OTSU segmentation

In hot images, the shadow reflected by the surface has an intensity that is close to the missing section of the image. So, in this case, the procedure to follow consists of performing an erosion of n iterations according to the image cluster, until these sections separate, and it is chosen to keep the section with the largest area. Finally, the section is dilated n times and added to the previous segmentation.

Fig. 6. Example of second RoI segmentation and shadow elimination

E. *Cable segmentation:*

The segmentation after the shadow elimination ignores key elements due to their lower contrast with respect to the background, and those are the cables. It is important to consider the cables in the segmentation because they provide important information about the status of the phases.

To identify them, the image is divided into regions in such a way that for the largest number of images the cables are in the same square region, and once this division is made, the Canny Edge Detector is used on those areas to find the cables.

Canny edge detection is a popular edge detection algorithm developed by John F. Canny that first removes noise using a 5x5 Gaussian filter.

As it is described in the OpenCV python library documentation [12] It then finds the intensity gradient of the image using a sobel kernel on both the X and Y axes. Then the first derivative is obtained in the horizontal and vertical direction.

Then follows the Non-maximum Suppression stage, in which all the pixels of the image are scanned and those that do not constitute the edges are removed. For this, it is checked if each pixel is a local maximum in its surroundings in the direction of the gradient. If it is a maximum, it is considered for the next stage, if not, its value changes to zero.

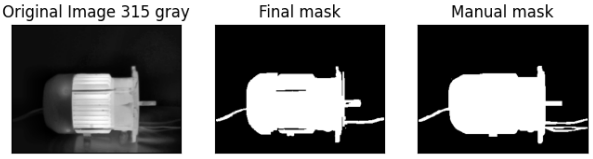

Fig. 7. Example of comparison between the original image, the mask generated by the algorithm and the manual mask

The final stage is the Hysteresis Thresholding stage, which defines which edges are truly edges and which are not. Two values are needed for this stage, a minimum and all pixels below that minimum are discarded, and a maximum and all pixels above that maximum are considered safe edges. Those that are between both values are classified as edges or non-edges based on their connectivity with neighboring pixels.

The precision of the masks generated by the previous process are measured with the Jaccard Score. This index compairs the similarity between the manual masks and its respective automated masks. The Basic Jaccard Index according to L. Fontura Costa [13] can simply be expresed as:

$$\mathcal{J}(A,B) = \frac{|A \cap B|}{|A \cup B|} = \frac{|A \cap B|}{|A| + |B| + |A \cap B|} \qquad (2)$$

Where A, and B are two sets. In this context, $|A \cap B|$ is the number of pixels of the image that have the same intensity, and $|A \cup B|$ is the size of the image. The results obtained for the 10 compared masks (one for each of the clusters) are between 0.73 and 0.81 for cold images and between 0.87 and 0.94 for hot images.

F. Classification

The methods proposed in the paper of the database have been explored considering the entire image once the pixels that are not part of the mask have been equaled to zero. However, the procedure has to be modified since the masks have different shapes and locations.

Taking this fact into account, it is key to find a way to vectorize and equalize the dimensionality of the arrays of regions of interest to implement the algorithms. The initial proposal to work on is to divide the images into regions according to the parts of the power system, and obtain general characteristics (mean, variance, minimum and maximum values, range, inertia, among others) and vectorize them to introduce them into supervised machine learning algorithms, especially tree-based ensemble classifiers.

V. Conclusions and further work

Work is currently underway to generalize the above procedure for multi-system cases in closed spaces and equipment failure monitoring located in open spaces. It is expected that in the near future results will be obtained for these other two types of monitoring, in such a way that the processes carried out for each of the cases can be compared, and thus establish algorithm guidelines for monitoring power systems with infrared images.

Acknowledgment

This work was funded by the IEEE Foundation Grant 94012 - IAS Zucker Faculty Grant 2022 ”Smart Industrial Power Systems with Advanced Data Analytics for Proactive and Predictive Maintenance” and it was partially funded by the starting grant IV-TFA056 entitled ”Machine learning for Smart Energy Systems” Research Direction at Universidad del Rosario. The authors would like to thank to the Center of Resources for Learning and Research (CRAI) at Universidad del Rosario for their help with the heuristic state-of-the-art for this manuscript.

References

[1] T. Ahmad, H. Zhu, D. Zhang, R. Tariq, A. Bassam, F. Ullah, A. S. AlGhamdi, and S. S. Alshamrani, “Energetics systems and artificial intelligence: Applications of industry 4.0,” *Energy Reports*, vol. 8, pp. 334–361, 2022. [Online]. Available: https://www.sciencedirect.com/science/article/pii/S2352484721014037

[2] A. S. Relkar, “Risk analysis of equipment failure through failure mode and effect analysis and fault tree analysis,” *Journal of Failure Analysis and Prevention*, vol. 21, no. 3, pp. 793–805, Jun 2021. [Online]. Available: https://doi.org/10.1007/s11668-021-01117-7

[3] V. Galaz, M. A. Centeno, P. W. Callahan, A. Causevic, T. Patterson, I. Brass, S. Baum, D. Farber, J. Fischer, D. Garcia, T. McPhearson, D. Jimenez, B. King, P. Larcey, and K. Levy, “Artificial intelligence, systemic risks, and sustainability,” *Technology in Society*, vol. 67, p. 101741, 2021. [Online]. Available: https://www.sciencedirect.com/science/article/pii/S0160791X21002165

[4] D. López-Pérez and J. Antonino-Daviu, “Application of infrared thermography to failure detection in industrial induction motors: Case stories,” *IEEE Transactions on Industry Applications*, vol. 53, no. 3, pp. 1901–1908, 2017.

[5] S. Han, F. Yang, H. Jiang, G. Yang, D. Wang, and N. Zhang, “Statistical analysis of infrared thermogram for cnn-based electrical equipment identification methods,” *Applied Artificial Intelligence*, vol. 36, no. 1, p. 2004348, 2022. [Online]. Available: https://doi.org/10.1080/08839514.2021.2004348

[6] L. Bommes, M. Hoffmann, C. Buerhop-Lutz, T. Pickel, J. Hauch, C. Brabec, A. Maier, and I. Marius Peters, “Anomaly detection in ir images of pv modules using supervised contrastive learning,” *Progress in Photovoltaics: Research and Applications*, vol. 30, no. 6, pp. 597–614, 2022. [Online]. Available: https://onlinelibrary.wiley.com/doi/abs/10.1002/pip.3518

[7] D. Manno, G. Cipriani, G. Ciulla, V. Di Dio, S. Guarino, and V. Lo Brano, “Deep learning strategies for automatic fault diagnosis in photovoltaic systems by thermographic images,” *Energy Conversion and Management*, vol. 241, p. 114315, 2021. [Online]. Available: https://www.sciencedirect.com/science/article/pii/S019689042100491X

[8] M. Najafi, Y. Baleghi, S. A. Gholamian, and S. Mehdi Mirimani, “Fault diagnosis of electrical equipment through thermal imaging and interpretable machine learning applied on a newly-introduced dataset,” in *2020 6th Iranian Conference on Signal Processing and Intelligent Systems (ICSPIS)*, 2020, pp. 1–7.

[9] E. Lucchi, “Applications of the infrared thermography in the energy audit of buildings: A review,” *Renewable and Sustainable Energy Reviews*, vol. 82, pp. 3077–3090, 2018. [Online]. Available: https://www.sciencedirect.com/science/article/pii/S1364032117314119

[10] M. Cubukcu and A. Akanalci, “Real-time inspection and determination methods of faults on photovoltaic power systems by thermal imaging in turkey,” *Renewable Energy*, vol. 147, pp. 1231–1238, 2020. [Online]. Available: https://www.sciencedirect.com/science/article/pii/S0960148119314065

[11] R. C. Gonzalez and R. E. Woods, *Image Segmentation: Thresholding*. Pearson, 2018.

[12] “Canny edge detection.” [Online]. Available: https://docs.opencv.org/4.x/da/d22/tutorial_py_canny.html

[13] L. da F. Costa, “Further generalizations of the jaccard index,” *CoRR*, vol. abs/2110.09619, 2021. [Online]. Available: https://arxiv.org/abs/2110.09619